

The **next generation** GBCA  
from Guerbet is here

Explore new possibilities >

Guerbet | 

© Guerbet 2024 GUOB220151-A

# AJNR

This information is current as  
of March 20, 2024.

## **Efficacy of Diffusion-Weighted Imaging for the Differentiation between Lymphomas and Carcinomas of the Nasopharynx and Oropharynx: Correlations of Apparent Diffusion Coefficients and Histologic Features**

Y. Ichikawa, M. Sumi, M. Sasaki, T. Sumi and T. Nakamura

*AJNR Am J Neuroradiol* 2012, 33 (4) 761-766

doi: <https://doi.org/10.3174/ajnr.A2834>

<http://www.ajnr.org/content/33/4/761>

ORIGINAL  
RESEARCH

Y. Ichikawa  
M. Sumi  
M. Sasaki  
T. Sumi  
T. Nakamura



# Efficacy of Diffusion-Weighted Imaging for the Differentiation between Lymphomas and Carcinomas of the Nasopharynx and Oropharynx: Correlations of Apparent Diffusion Coefficients and Histologic Features

**BACKGROUND AND PURPOSE:** ADCs may help distinguish benign from malignant head and neck diseases. We sought to evaluate the effectiveness of ADC for differentiating between carcinomas and lymphomas of the nasopharynx and oropharynx.

**MATERIALS AND METHODS:** We retrospectively compared the ADCs between 24 histologically proved lymphomas and 32 carcinomas, including 8 NPCs and 7 lymphomas of the nasopharynx, and 24 SCCs and 17 lymphomas of the oropharynx. ADCs were determined on tumor-by-tumor (overall ADCs) and pixel-by-pixel (ADC mapping) bases by using 2 b-values (500 and 1000 s/mm<sup>2</sup>).

**RESULTS:** Lymphomas and oropharyngeal SCCs had unique histologic features in terms of keratinization, cell attenuation, stromal areas, and necrosis and had distinctive ADCs ( $0.503 \pm 0.099 \times 10^{-3}$  mm<sup>2</sup>/s for lymphomas and  $0.842 \pm 0.164 \times 10^{-3}$  mm<sup>2</sup>/s for SCCs). However, NPCs and lymphomas were similar in terms of these histologic features, exhibiting comparable ADCs ( $0.567 \pm 0.057 \times 10^{-3}$  mm<sup>2</sup>/s for NPCs and  $0.528 \pm 0.094 \times 10^{-3}$  mm<sup>2</sup>/s for lymphomas). Poorly and moderately differentiated SCCs with homogeneous T2 signals were indistinguishable from lymphomas on conventional MR images; however, ADCs of these SCC subtypes were significantly larger than those of lymphomas. ADC mapping profiles with respect to percentage of tumor areas of extremely low, intermediate, and high ADC levels were well-correlated with the histologic features of lymphomas, NPCs, and different types of SCCs.

**CONCLUSIONS:** The effectiveness of ADC-based differentiation between lymphomas and carcinomas of the nasopharynx and oropharynx depends on their histologic characteristics.

**ABBREVIATIONS:** CV = coefficient of variance; NPC = nasopharyngeal carcinoma; SCC = squamous cell carcinoma; SENSE = sensitivity encoding; SPAIR = spectral-attenuated inversion recovery; SPIR = spectral presaturation with inversion recovery

The pharyngeal mucosal space is a common primary site for head and neck carcinomas and extranodal lymphomas. Lymphomas of nasopharynx and NPCs are typically centered in the adenoids and lateral pharyngeal recess. SCCs and lymphomas of the oropharynx usually arise from the palatine tonsil, lingual tonsil, and tongue base.

Lymphomas and carcinomas are staged differently on the basis of primary sites and/or tumor sizes.<sup>1</sup> High-quality imaging of these malignant tumors is important for tumor staging and treatment planning, and it is helpful if imaging can be performed before biopsy for histologic confirmation of the diagnosis. Histologic confirmation is necessary because it is often difficult to clinically differentiate between lymphomas and carcinomas of the nasopharynx and oropharynx on the basis of conventional MR imaging alone. For example, some carcinomas are heterogeneous on conventional MR images,

but others are homogeneous and thus resemble lymphomas. Previous studies demonstrated that ADCs can be used to effectively differentiate between metastatic SCC nodes and lymphoma nodes in the neck.<sup>2,3</sup> Therefore, ADC-based differentiation between lymphomas and carcinomas should be effective. However, another study showed that ADCs of some types of pharyngeal carcinomas (ie, poorly differentiated SCCs) significantly overlap those of lymphomas.<sup>4</sup> Therefore, ADC-based differentiation between these malignancies may be ineffective. In addition, it is not well-understood why some types of carcinomas cannot be differentiated on the basis of ADCs.

NPCs encompass nonkeratinizing carcinoma (differentiated and undifferentiated), keratinizing SCC, and basaloid SCC. Of the NPCs, 75%–99% are nonkeratinizing carcinomas, which are histologically characterized by sheets of crowded carcinoma cells separated by an attenuated infiltrate of lymphocytes and plasma cells.<sup>5</sup> Many oropharyngeal SCCs are moderately differentiated or well-differentiated, with only 20% showing poorly differentiated characteristics.<sup>6</sup> Therefore, with respect to tissue cellularity, most carcinomas in the nasopharynx and a significant number of carcinomas in the oropharynx may have histologic characteristics akin to those of lymphomas. The extracellular-to-intracellular ratio is a major

Received May 19, 2011; accepted after revision July 8.

From the Department of Radiology and Cancer Biology, Nagasaki University School of Dentistry, Nagasaki, Japan.

Please address correspondence to Takashi Nakamura, DDS, PhD, Department of Radiology and Cancer Biology, Nagasaki University School of Dentistry, Sakamoto 1-7-1, Nagasaki 852-8588, Japan; e-mail: taku@nagasaki-u.ac.jp

 Indicates article with supplemental on-line tables.

<http://dx.doi.org/10.3174/ajnr.A2834>

determinant of tissue ADCs.<sup>7</sup> Thus, ADC-based differentiation between lymphomas and carcinomas of the nasopharynx and oropharynx might not be feasible.

The present study aims to evaluate the efficacy of ADC-based differentiation between lymphomas and carcinomas of the nasopharynx and oropharynx. To this end, we assessed ADCs of these malignant diseases on tumor-by-tumor (overall ADCs) and pixel-by-pixel (ADC mapping) bases and compared the obtained ADCs with histologic features between lymphomas and different histologic types of carcinomas.

## Materials and Methods

### Patients

The study protocol was approved by the institutional review board, and written informed consent was obtained from all patients. DWI from 60 patients with histologically proved lymphoma or carcinoma in the nasopharynx or oropharynx was retrospectively reviewed. These patients underwent both conventional and DWI before endoscopic biopsy from April 2003 to October 2010. Endoscopic biopsy was used in all cases. Of these, the diseased site was not detectable on MR images in 1 patient with carcinoma in the nasopharynx, and MR images were judged poor due to significant artifacts in 3 patients with carcinoma in the oropharynx. Consequently, we studied MR images (fat-suppressed T2-weighted images and DWI) of 56 patients (7 patients with lymphoma of the nasopharynx, 17 with lymphoma of the oropharynx, 8 with carcinoma of the nasopharynx, and 24 with carcinoma of the oropharynx). The average age of the 56 patients was  $63 \pm 16$  years (22 women and 34 men;  $68 \pm 19$  years for patients with lymphoma and  $60 \pm 13$  years for those with carcinoma).

Of the NPCs, 4 were differentiated and 4 were undifferentiated nonkeratinizing carcinomas. Of the SCCs of the oropharynx, 9 were poorly differentiated, 8 were moderately differentiated, and 7 were well-differentiated. The lymphomas included 1 T-cell and 6 B-cell tumors of the nasopharynx and 15 B-cell and 2 T-cell tumors of the oropharynx.

### MR Imaging

MR imaging was performed by using a 1.5T scanner (Gyrosan Intera 1.5T Master; Philips, Best, the Netherlands) with a 200-mm Synergy Flex L Coil, a  $140 \times 170$  mm Synergy Flex M Coil, or a Synergy Head/Neck Coil (Philips). Imaging was performed by using a 200-mm FOV, 4- to 5-mm section thickness, and a 0.8- to 1.0-mm section gap. To compensate for the image intensity inhomogeneity, we used the Constant Level Appearance postprocessing technique (Philips).

### Conventional MR Imaging

We obtained conventional T1-weighted (TR/TE/number of signal intensity acquisitions = 500 ms/14 ms/2) and fat-suppressed (SPIR or SPAIR) T2-weighted (TR/TE/number of signal intensity acquisitions = 4784 ms/80 ms/2 for SPIR; 6385 ms/80 ms/2 for SPAIR) axial MR images by using a turbo spin-echo sequence. We used a  $256 \times 256$  matrix size.

### DWI

Axial DWI (TR/TE/number of signal intensity acquisitions = 4286 ms/87 ms/4) was obtained with a single-shot spin-echo echo-planar imaging sequence. The reconstruction matrix size was  $256 \times 256$ . We used a parallel imaging technique (SENSE technique, SENSE factor =

2) to prevent susceptibility artifacts with reduction in echo-train length during the DWI. To minimize effects by perfusion in tumor tissues, we determined ADCs by using 2 high b factors (500 and 1,000 s/mm<sup>2</sup>). Isotropic diffusion images were obtained, with the 2 b factors applied along the 3 orthogonal directions. This procedure requires additional time to perform, but the combined use of the SENSE technique allowed us to obtain DWI without significant motion artifacts. The total image-acquisition time was 2 minutes 8 seconds/25 sections by using the SENSE technique.

### Analysis of Fat-Suppressed T2-Weighted MR Images

Fat-suppressed T2-weighted MR images (3 middle images from each tumor) were qualitatively and quantitatively analyzed with respect to heterogeneous or homogeneous tumor signals. Tumor heterogeneity on T2-weighted images was quantitatively analyzed by calculating CV as the following:  $CV (\%) = (SD \text{ of signal intensities in tumor area}) \times 100 / (\text{mean signal intensity of tumor area})$ . Therefore, a tumor having a higher CV indicates a tumor with more heterogeneous T2 signals.

### Analysis of DWI

ADCs were determined on tumor-by-tumor (overall ADCs) and pixel-by-pixel (ADC mapping) bases. Gray-scale ADC map images (3 middle images from each tumor) were saved in DICOM format. Free-hand ROIs along the margins of the lesions were manually placed onto the ADC maps by using the corresponding fat-suppressed T2-weighted MR images as references for placing the ROIs (Fig 1). Then, average ADCs of the whole lesions were determined (overall ADCs).

For ADC mapping, the gray-scale ADC maps, on which lesions were indicated by ROIs, were converted to color ADC map images after setting the window level of gray-scale ADC map images at 1300 and the window width at 2600. As a result, tumor areas having high ADCs were displayed as color areas of long wavelengths such as red, and tumor areas having low ADCs were displayed as color areas of short wavelengths such as blue (Fig 1). These procedures were performed on a personal computer by using OsiriX software (<http://www.osirix-viewer.com/>).<sup>8</sup>

We classified the tumor areas into 4 categories on the basis of ADC level, as previously described (Fig 1).<sup>9</sup> In brief, we determined the tumor area having extremely low ADC ( $< 0.6 \times 10^{-3}$  mm<sup>2</sup>/s), low ADC ( $0.6 \times 10^{-3}$  mm<sup>2</sup>/s  $\leq$  ADC  $< 1.2 \times 10^{-3}$  mm<sup>2</sup>/s), intermediate ADC ( $1.2 \times 10^{-3}$  mm<sup>2</sup>/s  $\leq$  ADC  $< 1.8 \times 10^{-3}$  mm<sup>2</sup>/s), or high ADC ( $\geq 1.8 \times 10^{-3}$  mm<sup>2</sup>/s) relative to the total lesion on ADC maps by using ImageJ software (<http://rsbweb.nih.gov/ij/>) and expressed these as percentage areas.

### Interobserver and Intraobserver Agreement for ADC Determination

Reproducibility of ADC measurements is a critical factor. Gordon et al<sup>10</sup> reported that MR imaging-based volume measurements of pharyngeal carcinomas are reliably reproducible, with a mean percentage error of 12% for the measurements. Therefore, poor reproducibility in the placement of ROIs would greatly affect the reliability of the ADC measurement. In the pilot study, we assessed the interobserver and intraobserver errors in ADC measurements by using a small number of cases from the present study cohort (4 lymphomas and 8 carcinomas). We found that the average interobserver error was 3.7% CV (SD of ADC  $\times 100/\text{mean ADC}$ ), and the average intraobserver error was 3.3% CV. These errors were smaller than those reported in the volume measurements of pharyngeal SCCs,<sup>10</sup> suggesting that

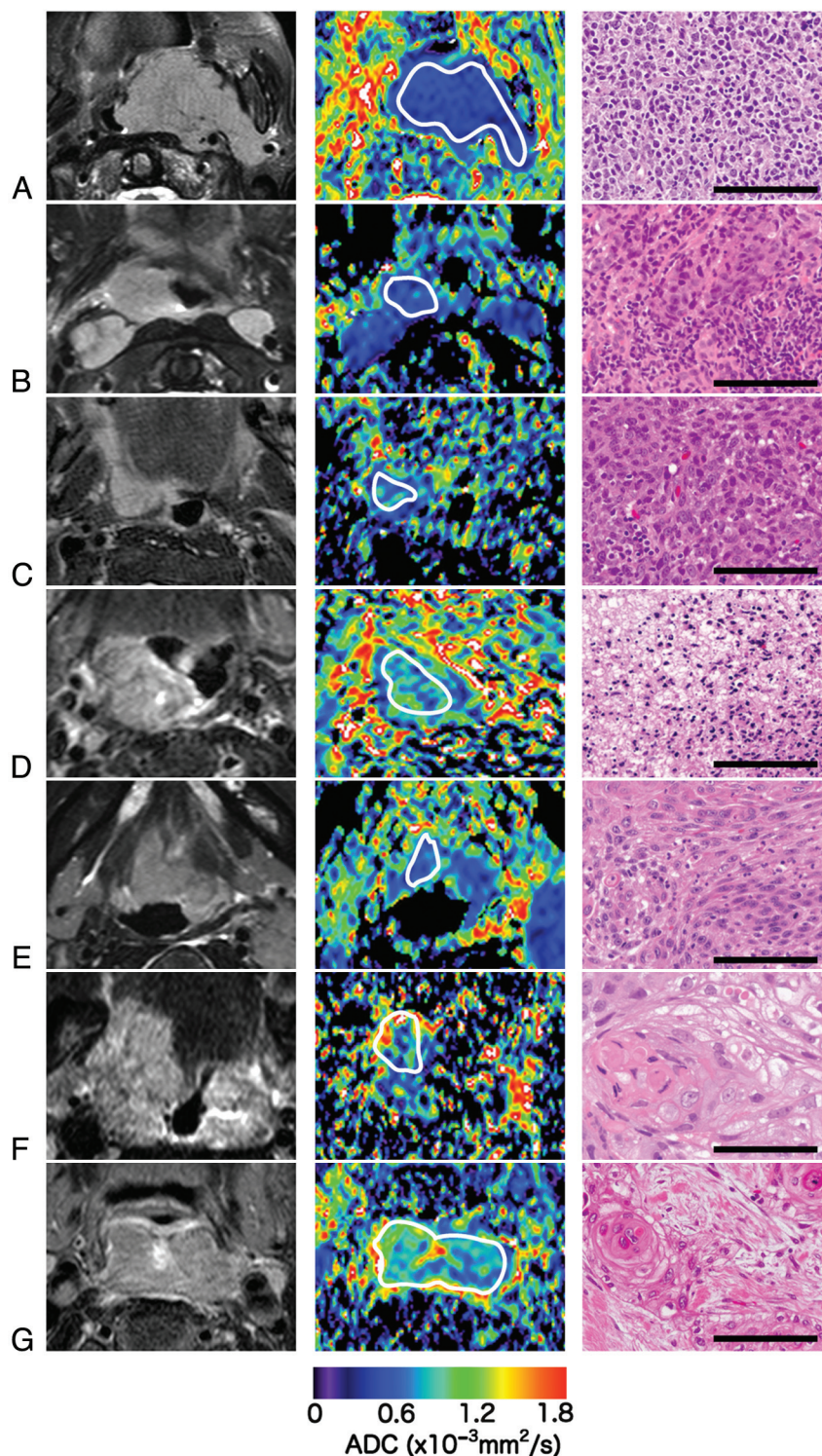


**Fig 1.** Axial fat-suppressed T2-weighted images (left panels), color ADC maps (middle panels), and photomicrographs (right panels) of lymphomas and carcinomas of the nasopharynx and oropharynx. *A*, A 92-year-old woman with oropharyngeal lymphoma (overall ADC =  $0.558 \times 10^{-3} \text{ mm}^2/\text{s}$ ; ADC mapping = 79%, extremely low; 21%, low; 0%, intermediate; and 0%, high). *B*, A 49-year-old woman with NPC (overall ADC =  $0.566 \times 10^{-3} \text{ mm}^2/\text{s}$ ; ADC mapping = 55%, extremely low; 45%, low; 0%, intermediate; and 0%, high). *C*, A 52-year-old man with poorly differentiated SCC exhibiting homogeneous T2 signals (overall ADC =  $0.576 \times 10^{-3} \text{ mm}^2/\text{s}$ ; ADC mapping = 21%, extremely low; 78%, low; 1%, intermediate; and 0%, high). *D*, A 66-year-old man with poorly differentiated SCC exhibiting heterogeneous T2 signals (overall ADC =  $1.02 \times 10^{-3} \text{ mm}^2/\text{s}$ ; ADC mapping = 4%, extremely low; 65%, low; 31%, intermediate; and 1%, high). *E*, A 67-year-old man with moderately differentiated SCC exhibiting homogeneous T2 signals (overall ADC =  $0.752 \times 10^{-3} \text{ mm}^2/\text{s}$ ; ADC mapping = 22%, extremely low; 77%, low; 1%, intermediate; and 0%, high). *F*, A 62-year-old man with moderately differentiated SCC exhibiting heterogeneous T2 signals (overall ADC =  $0.904 \times 10^{-3} \text{ mm}^2/\text{s}$ ; ADC mapping = 21%, extremely low; 61%, low; 15%, intermediate; and 3%, high). *G*, A 66-year-old man with well-differentiated SCC (overall ADC =  $0.975 \times 10^{-3} \text{ mm}^2/\text{s}$ ; ADC mapping = 5%, extremely low; 83%, low; 12%, intermediate; and 1%, high). The color scale for ADC mapping is shown at the bottom. White curvilinear lines indicate ROIs. Bars in photomicrographs (H&E) are scale bars (50  $\mu\text{m}$ ).

ADC measurement of nasopharyngeal and oropharyngeal tumors is reliably reproducible.

### Histologic Assessment

Histologic findings of excised specimens obtained at endoscopic biopsy and/or at surgery were compared with ADC levels in the lymphomas and carcinomas. Direct comparison between histologic sections and the corresponding DWI maps of tumors was not achievable because in most cases, the specimens were obtained at biopsy (eg, in all the lymphomas and NPCs) and the planes of MR images and those of histologic sections in each tumor were not identical. Therefore, we qualitatively characterized the histology in terms of the following: 1) cell attenuation (low, intermediate, or high), 2) amount of stromal tissue area (faint,  $\pm$ ; intermediate,  $+$ ; or abundant,  $++$ ), 3) the presence ( $++$ ) or absence ( $-$ ) of necrosis, and 4) the presence ( $++$ ) or absence ( $-$ ) of keratinized deposits. The final estimation was made by consensus of 2 observers. Obtained data are summarized for each tumor group (On-line Table 1).

### Statistical Analysis

The significance of differences in overall ADCs, ADC mapping profiles, and percentage CVs of signal intensity between the different tumor groups was assessed by the Mann-Whitney *U* test.

## Results

### T2-Weighted MR Imaging

All lymphomas and NPCs were homogeneous on fat-suppressed T2-weighted images (On-line Table 2 and Fig 1). In contrast, all well-differentiated SCCs were heterogeneous. More than half (56%) of poorly differentiated SCCs and approximately one-third (38%) of moderately differentiated SCCs were homogeneous on fat-suppressed T2-weighted images.

### Overall ADCs of Lymphomas and Carcinomas

In the oropharynx, the overall ADCs of lymphomas ( $0.503 \pm 0.099 \times 10^{-3} \text{ mm}^2/\text{s}$ ) were significantly smaller than those of carcinomas ( $0.842 \pm 0.164 \times 10^{-3} \text{ mm}^2/\text{s}$ ) (Fig 2). The best cutoff ADC was  $0.66 \times 10^{-3} \text{ mm}^2/\text{s}$ , which discriminated oropharyngeal lymphomas from SCCs with 100% sensitivity, 88% specificity, 93% accuracy, and 85% positive and 100% negative predictive values. In contrast, the overall ADCs were similar between nasopharyngeal lymphomas ( $0.528 \pm 0.094 \times 10^{-3} \text{ mm}^2/\text{s}$ ) and NPCs ( $0.567 \pm 0.057 \times 10^{-3} \text{ mm}^2/\text{s}$ ) (Fig 2).

### Correlations between Overall ADCs and Histologic Features of Lymphomas and Carcinomas

All 8 NPCs were nonkeratinized carcinomas, and their histologic features were indistinguishable from those of lymphomas in terms of cell attenuation and the amounts of stromal tissues, necrosis, and keratinization (On-line Table 1 and Fig 1). All of the oropharyngeal carcinomas were keratinized SCCs. The cell attenuation was lower, and the amounts of stromal tissues, necrosis, and keratinized deposits were higher in well-differentiated SCCs than in SCCs with lower differentiation subtypes with homogeneous T2 signals (On-line Table 1, Fig 1). Poorly and moderately differentiated SCCs with het-

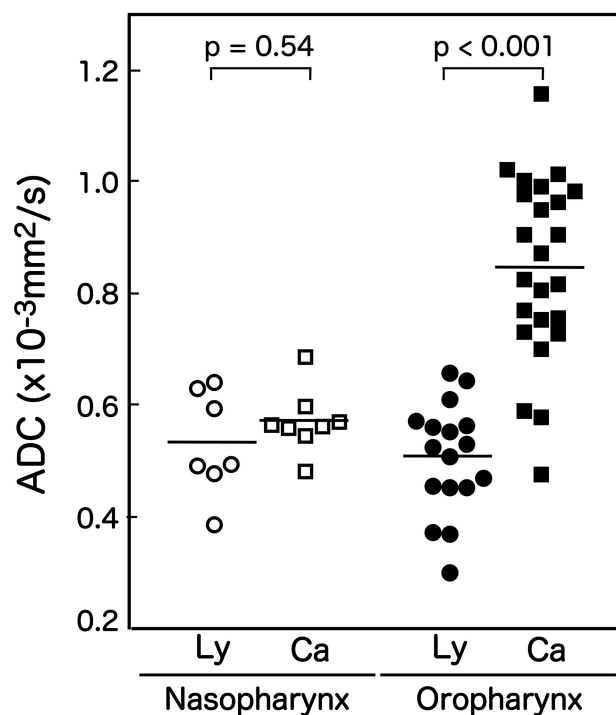


**Fig 2.** Scatterplot shows overall ADCs of lymphomas and carcinomas of the nasopharynx or oropharynx. Ly indicates lymphomas; Ca, carcinomas. Horizontal bars indicate mean ADCs (*P* value, Mann-Whitney *U* test).

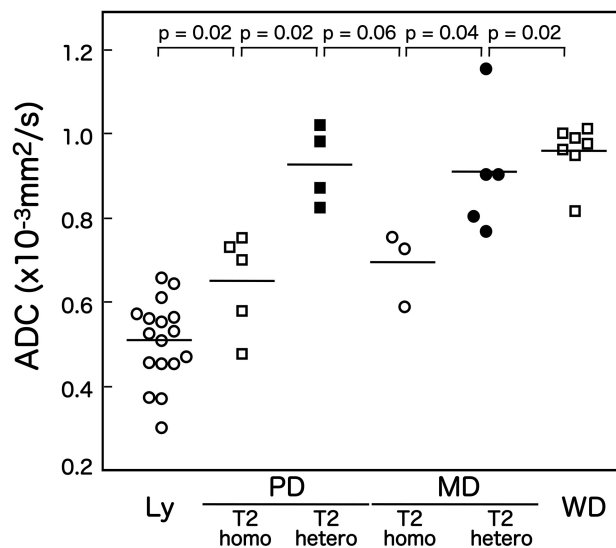


**Fig 3.** Scatterplot shows overall ADCs of lymphomas and carcinomas with different histologic subtypes. Ly indicates lymphomas; PD, poorly differentiated SCCs with homogeneous T2 signals (T2 homo) or heterogeneous T2 signals (T2 hetero); MD, moderately differentiated SCCs with homogeneous T2 signals (T2 homo) or heterogeneous T2 signals (T2 hetero); WD, well-differentiated SCCs. Horizontal bars indicate mean ADCs (*P* value, Mann-Whitney *U* test).

erogeneous T2 signals contained more stromal tissue and necrotic areas than those with homogeneous T2 signals.

The overall ADCs correlated well with the histology of the carcinomas and lymphomas (On-line Table 1 and Figs 2 and 3). Lymphomas and NPCs had the smallest ADCs, whereas well-differentiated SCCs had the largest ADCs ( $0.957 \pm 0.067 \times 10^{-3} \text{ mm}^2/\text{s}$ ). Poorly differentiated SCCs with homogeneous T2 signals exhibited significantly lower ADCs

# ADC mapping of lymphomas and carcinomas in the nasopharynx and oropharynx

ADC Mapping ( $\times 10^{-3} \text{ mm}^2/\text{s}$ )	Percentage of Tumor Area on ADC Map							
	Nasopharynx		Oropharynx					
	Lymphoma	NPC	Lymphoma	PD SCC		MD SCC		WD SCC
				T2 Homo	T2 Hetero	T2 Homo	T2 Hetero	
No. of patients	7	8	17	5	4	3	5	7
Extremely low ( $<0.6$ )	$68 \pm 15$	$57 \pm 12$	$51 \pm 35^{a,b,c,d}$	$34 \pm 25$	$10 \pm 5^{a,b}$	$24 \pm 25$	$15 \pm 13^{a,c}$	$15 \pm 22^{a,d}$
Low ( $0.6\text{--}1.2$ )	$32 \pm 14$	$43 \pm 12$	$48 \pm 34$	$64 \pm 25$	$74 \pm 7$	$75 \pm 26$	$68 \pm 18$	$63 \pm 14$
Intermediate ( $1.2\text{--}1.8$ )	$0 \pm 0$	$1 \pm 1$	$1 \pm 2^{a,e,f}$	$1 \pm 2^{a,g}$	$16 \pm 10^{a,e,g}$	$2 \pm 2$	$15 \pm 19^{a,f}$	$19 \pm 15$
High ( $>1.8$ )	$0 \pm 0$	$0 \pm 0$	$0 \pm 0$	$0 \pm 0$	$0 \pm 0$	$0 \pm 0$	$2 \pm 3$	$3 \pm 5$

**Note:**—PD, poorly differentiated; MD, moderately differentiated; Homo, homogeneous; Hetero, heterogeneous; WD, well-differentiated; T2 homo/hetero, with homogeneous/heterogeneous T2 signals.

<sup>a</sup> Significant differences between lymphomas and SCCs, and between PD SCCs with homogeneous T2 signals and heterogeneous T2 signals (Mann-Whitney *U* test).

<sup>b</sup>  $P = .040$ .

<sup>c</sup>  $P = .048$ .

<sup>d</sup>  $P = .011$ .

<sup>e</sup>  $P = .001$ .

<sup>f</sup>  $P < .001$ .

<sup>g</sup>  $P = .019$ .

( $0.645 \pm 0.118 \times 10^{-3} \text{ mm}^2/\text{s}$ ) than those with heterogeneous T2 signals ( $0.923 \pm 0.092 \times 10^{-3} \text{ mm}^2/\text{s}$ ) (Fig 3). Similarly, moderately differentiated SCCs with homogeneous T2 signals had significantly lower ADCs ( $0.688 \pm 0.089 \times 10^{-3} \text{ mm}^2/\text{s}$ ) than those with heterogeneous T2 signals ( $0.906 \pm 0.152 \times 10^{-3} \text{ mm}^2/\text{s}$ ). However, ADCs of poorly and moderately differentiated SCCs with homogeneous T2 signals were significantly higher than those of lymphomas ( $0.503 \pm 0.099 \times 10^{-3} \text{ mm}^2/\text{s}$ ).

## ADC Mapping of Lymphomas and Carcinomas

Pixel-based ADC mapping allowed us to investigate the 2D distribution of ADCs in each tumor (Fig 1). Nasopharyngeal lymphomas and NPCs exhibited similar distributions of extremely low, low, intermediate, and high ADC areas (Table). Poorly and moderately differentiated SCCs with heterogeneous T2 signals contained significantly smaller areas of extremely low ADCs and significantly larger areas of intermediate ADCs than did lymphomas (Table). However, ADC mapping profiles of SCCs with homogeneous T2 signals were close to those of lymphomas in terms of tumor areas with extremely low and intermediate ADCs (Table).

## Discussion

In this preliminary study, we evaluated the effectiveness of ADC-based differentiation between lymphomas and carcinomas of the nasopharynx and oropharynx. We found that ADC-based differentiation of lymphomas from carcinomas was effective in the oropharynx, but not in the nasopharynx. A major reason for this discrepancy is very likely because nasopharyngeal carcinomas have histologic features similar to lymphomas in terms of high cell attenuation, absence of keratinization, and scarce amounts of stromal and necrotic tissues (Fig 1 and On-line Table 1). In contrast, the keratinized SCCs of the oropharynx contain large areas of stromal tissues and scattered areas of necrosis; these tissue components have relatively high ADC values. Furthermore, we found that ADC levels were also correlated with differential histology within the same types of SCCs.

NPCs are histologically categorized into 3 types: nonkeratinizing carcinomas, keratinizing SCCs, and basaloid SCCs.<sup>5</sup>

Nonkeratinizing carcinomas comprise solid sheets of carcinoma cells closely intermingled with varying numbers of lymphocytes and plasma cells; in some cases, abundant lymphocytes and plasma cells infiltrate the sheets of carcinomas, breaking them into tiny epithelial islands. Small ADCs observed in the 8 cases of nonkeratinizing carcinoma presented in this study might be because of such histologic features of lymphoepithelial carcinoma. On the other hand, keratinizing SCCs, the second frequent subtype of NPC, have an abundant desmoplastic stroma infiltrated by varying numbers of lymphocytes and plasma cells. The present study cohort did not include this NPC subtype. However, these keratinizing SCCs are histologically similar to keratinizing SCCs occurring in the oropharynx. Therefore, if keratinizing SCCs were included in the present study cohort, their differentiation would be similar to that observed in the SCCs of the oropharynx.

Therefore, a small but statistically significant difference in ADCs between lymphomas and NPCs might be detected in a large patient cohort that contains many patients with keratinizing SCCs.

Consistent with the results of a previous study, we demonstrated that ADCs and degrees of differentiation were closely related to differential histology in oropharyngeal SCCs.<sup>4</sup> Furthermore, we found that poorly differentiated SCCs can be subdivided into 2 types on the basis of fat-suppressed T2-weighted images, namely, poorly differentiated SCCs with homogeneous T2 signals and those with heterogeneous T2 signals. Poorly differentiated SCCs with homogeneous T2 signals had significantly smaller ( $<0.8 \times 10^{-3} \text{ mm}^2/\text{s}$ ) ADCs than those with heterogeneous T2 signals (Fig 3). These results are consistent with the histologic findings that poorly differentiated SCCs with heterogeneous T2 signals contained larger areas of necrosis and stromal tissues than did poorly differentiated SCCs with homogeneous T2 signals (On-line Table 1). However, the ADC levels of poorly differentiated SCCs with homogeneous T2 signals were significantly larger than those of lymphomas in the oropharynx (Fig 3). These results are consistent with the notion that the presence of necrosis greatly influences the ADC levels of the tissue.<sup>9,11,12</sup> Thus, these results suggest the usefulness of ADC measurement for differen-

tiation between lymphomas and SCC subtypes of the oropharynx.

Results obtained by ADC mapping are well-correlated with the histologic features of the lymphomas, NPCs, and SCCs (Table). In the present study, we were not able to directly correlate histologic findings and ADC maps of the tumors because histologic sections that correspond to the DWI were not available, as mentioned in the "Materials and Methods" section. However, previous studies demonstrated that tumor areas with extremely low ADCs represent densely packed cell-rich components, tumor areas with low ADCs represent fibrous stromal tissues associated with cancer nests, areas with intermediate ADCs represent abundant stromal tissues, and areas with high ADCs represent necrotic or cystic components.<sup>13</sup> Consistent with these notions, the areas having extremely low ADCs decrease and those having low or intermediate ADCs increase in SCCs with higher differentiation subtypes. The tumor areas with high ADCs are evident in moderately and well-differentiated SCCs but not in poorly differentiated SCCs, indicating increased areas of necrosis in SCCs with higher differentiation subtypes (Table). The presence of keratinized deposits may reduce the tissue ADC levels.<sup>14</sup> ADC mapping confirms that lymphomas and nonkeratinized NPCs have indistinguishable ADC profiles.

ADC levels of tumors with high T2 signals are often high. Actually, several studies on head and neck tumors identified significant differences in ADC levels, which were correlated to T2 signal intensity levels.<sup>4,14</sup> However, the ADC is defined independent of T2 signals. In the present study, ADCs of poorly and moderately differentiated SCCs with homogeneous T2 signals were significantly larger than those of lymphomas (Fig 3). These results suggest that the presence of microscopic areas of necrosis in these SCCs with homogeneous T2 signals were attributed to the observed differences in ADC between poorly or moderately differentiated SCCs and lymphomas. Therefore, ADC measurement may be of added benefit to T2 signal-intensity evaluation for discriminating SCCs from lymphomas of the nasopharynx and oropharynx.

A major drawback of this study is the small study cohort. Therefore, the effectiveness of ADC-based differentiation between lymphomas and carcinomas of the nasopharynx and oropharynx should be decisively determined after conducting further studies on larger cohorts. The lack of direct correlation between MR images and histologic sections is an additional flaw of this study. Another apparent weakness of this study is that significant overlaps in ADC were present between lymphomas and carcinomas, even in the oropharynx. Assessment of the possible differences in perfusion between the lymphomas and carcinomas would be useful for facilitating differentiation between these 2 malignant diseases.<sup>15</sup>

The present study demonstrates that ADC measurement is helpful for preoperative diagnosis of lymphomas and carcino-

mas in the oropharynx. However, lymphomas and carcinomas of the nasopharynx cannot be differentiated by conventional MR imaging or DWI. In addition, a significant overlap in ADCs is still present between lymphomas and carcinomas of the oropharynx. Therefore, the confirmation of these diseases in the nasopharynx and oropharynx depends on tissue sampling.<sup>3,16</sup>

## Conclusions

In this patient cohort, ADC could be used to differentiate lymphomas from carcinomas in the oropharynx but not in the nasopharynx. The effectiveness of ADC-based differentiation of lymphomas from carcinomas of the nasopharynx and oropharynx depends largely on differential histology of these malignant tumors, and thus the differentiation between lymphomas and NPCs is ineffective because of the similar histologic features of these malignant tumors.

## References

1. Sobin LH, Wittekind C, eds. *TNM Classification of Malignant Tumours*. New York: Wiley-Liss; 2002
2. Sumi M, Sakihama N, Sumi T, et al. Discrimination of metastatic cervical lymph nodes with diffusion-weighted MR imaging in patients with head and neck cancer. *AJNR Am J Neuroradiol* 2003;24:1627-34
3. Vandecaveye V, De Keyser F, Vander Poorten V, et al. Head and neck squamous cell carcinoma: value of diffusion-weighted MR imaging for nodal staging. *Radiology* 2009;251:134-46
4. Sumi M, Ichikawa Y, Nakamura T. Diagnostic ability of apparent diffusion coefficients for lymphomas and carcinomas in the pharynx. *Eur Radiol* 2007;17:2631-37
5. Barnes L, Eveson JW, Reichart P, et al, eds. *Pathology and Genetics of Head and Neck Tumors; IARC WHO Classification of Tumours*. Lyon: IARC Press; 2005
6. Cohan DM, Popat S, Kaplan SE, et al. Oropharyngeal cancer: current understanding and management. *Curr Opin Otolaryngol Head Neck Surg* 2009;17:88-94
7. Le Bihan D. Looking into the functional architecture of the brain with diffusion MRI. *Nat Rev Neurosci* 2003;4:469-80
8. Rosset A, Spadola L, Ratib O. OsiriX: an open-resource software for navigating in multidimensional DICOM images. *J Digit Imaging* 2004;17:205-16
9. Eida S, Sumi M, Sakihama N, et al. Apparent diffusion coefficient mapping of salivary gland tumors: prediction of the benignancy and malignancy. *AJNR Am J Neuroradiol* 2007;28:116-21
10. Gordon AR, Loevner LA, Shukla-Dave A, et al. Intraobserver variability in the MR determination of tumor volume in squamous cell carcinoma of the pharynx. *AJNR Am J Neuroradiol* 2004;25:1092-98
11. Le Bihan D, Breton E, Lallemand D, et al. MR imaging of intravoxel incoherent motions: application to diffusion and perfusion in neurologic disorders. *Radiology* 1986;161:401-07
12. Sumi M, Nakamura T. Diagnostic importance of focal defects in the apparent diffusion coefficient-based differentiation between lymphoma and squamous cell carcinoma nodes in the neck. *Eur Radiol* 2009;19:975-81
13. Nakamura T, Sumi M, Van Cauteren M. Salivary gland tumors: preoperative tissue characterization with apparent diffusion coefficient mapping. In: Hayat M, ed. *Methods of Cancer Diagnosis, Therapy, and Prognosis, Vol. 2*. New York: Springer-Verlag; 2010:255-69
14. Sumi M, Ichikawa Y, Katayama I, et al. Diffusion-weighted MR imaging of ameloblastomas and keratocystic odontogenic tumors: differentiation by apparent diffusion coefficients of cystic lesions. *AJNR Am J Neuroradiol* 2008;29:1897-901. Epub 2008 Aug 21
15. Le Bihan D. Intravoxel incoherent motion perfusion MR imaging: a wake-up call. *Radiology* 2008;249:748-52
16. Wei WI, Kwong DL. Current management strategy of nasopharyngeal carcinoma. *Clin Exp Otorhinolaryngol* 2010;1:1-12